

Size of orbital-ordering domain controlled by the itinerancy of the 3d electrons in a manganite thin film

Y. Wakabayashi,^{1,2} H. Sagayama,³ T. Arima,³ M. Nakamura,^{4,*} Y. Ogimoto,^{5,6} Y. Kubo,⁵ K. Miyano,^{5,6} and H. Sawa^{1,7}

¹Photon Factory, Institute of Materials Structure Science, High Energy Accelerator Research Organization, Tsukuba 305-0801, Japan

²Graduate School of Engineering Science, Osaka University, Toyonaka 560-8531, Japan

³IMRAM, Tohoku University, Sendai 980-8577, Japan

⁴Department of Applied Physics, University of Tokyo, Tokyo 113-8586, Japan

⁵Research Center for Advanced Science and Technology, University of Tokyo, Tokyo 153-8904, Japan

⁶CREST, Japan Science and Technology Agency, Honcho 4-1-8, Kawaguchi 332-0012, Japan

⁷Department of Applied Physics, Nagoya University, Nagoya 464-8603, Japan

(Received 13 April 2009; published 10 June 2009)

An electronic effect on a macroscopic domain structure is found in a strongly correlated half-doped manganite film $\text{Nd}_{0.5}\text{Sr}_{0.5}\text{MnO}_3$ grown on a (011) surface of SrTiO_3 . The sample has a high-temperature (HT) phase free from distortion above 180 K and two low-temperature (LT) phases with a large shear-mode strain and a concomitant twin structure. One LT phase has a large itinerancy (A type), and the other has a small itinerancy (CE type), while the lattice distortions they cause are almost equal. Our x-ray diffraction measurement shows that the domain size of the LT phase made by the HT-CE transition is much smaller than that by the HT-A transition, indicating that the difference in domain size is caused by the difference in orbital arrangement and resulting itinerancy of the LT phases.

DOI: [10.1103/PhysRevB.79.220403](https://doi.org/10.1103/PhysRevB.79.220403)

PACS number(s): 75.70.-i, 64.75.St, 75.47.Lx

Macroscopic domain structures, such as magnetic ones, martensites, and lamella or gyroid structures of liquid crystals, abound in various materials. While the properties of each domain's constituents are often dominated by short-range interactions such as exchange interactions, the macroscopic shape and size of the domain are usually dominated by long-range interactions, such as static electromagnetic interactions or stress, because the effect of the long-range interactions accumulates as the domain grows.

Many manganites also show lamella-type domain structures in their orbital ordered phases.^{1,2} Although the orbital ordering itself is a manifestation of the strong correlation among the electrons,³ the domain structure is primarily dominated by local stress.¹ We have found, in contrast to this, a significant change in the macroscopic domain structure caused by a change in the itinerancy of the 3d electrons in a $\text{Nd}_{0.5}\text{Sr}_{0.5}\text{MnO}_3$ thin film on a $\text{SrTiO}_3(011)$ substrate (NSMO/STO) through x-ray diffraction measurements under magnetic fields. Since this change in domain structure is made by applying the magnetic field, most of the extrinsic effects such as nucleation caused by different density of chemical defects are excluded. From a materials science stand point, good understanding of the domain structure gives us further insights into the macroscopic material properties of strongly correlated systems because the percolative phenomena are often observed in various strongly correlated materials.⁴

The orbital states of e_g electrons are best studied by examining structural properties because of the strong coupling between the e_g electrons and the lattice.⁵ This coupling makes a lattice strain when charge and orbital ordering occur,⁶ and the strain may cause a phase coexistence in some cases.⁷ Our previous study on NSMO/STO under zero field⁸⁻¹⁰ shows that this film has a ferromagnetic (FM) phase below 210 K, x^2-y^2 -type ferro-orbital ordered phase (A-OO

phase) below $T_A=180$ K, and $3x^2-r^2/3y^2-r^2$ antiferro-orbital ordered phase (CE-OO phase) below $T_{CE}=160$ K. There are two kinds of twin structures. One is related to the film growth—that is, to the tilt of the a^* axis in $[011]$ direction by $\pm 0.4^\circ$ (twin-1)—and the other happens at T_A at which the b and c lattice parameters split (twin-2, see the inset of Fig. 1). Throughout this Rapid Communication, we use cubic notation of the lattice parameters for the sake of direct comparison with references.^{9,10} From the view point of structural deformation, we call the phase having the relation $b=c$ as the HT phase (paramagnetic and FM phases) and $b \neq c$ as the low-temperature (LT) phase (A-OO and CE-OO phases). The HT-LT transition at T_A is a kind of martensitic transition,⁶ which changes the lattice parameters without making a diffusion of the atoms, as well as a Jahn-Teller transition. The metal-insulator transition temperature T_{MI} co-

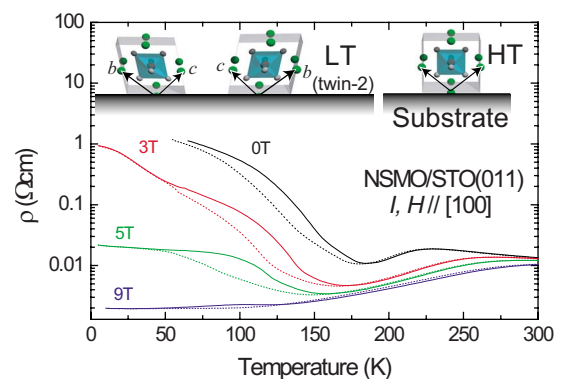


FIG. 1. (Color online) Temperature dependence of the resistivity in various magnetic fields. Solid curves and dashed curves show the results on warming and cooling runs, respectively. Inset: schematic view of high-temperature (HT) phase and two twin-2 structures with shear-mode strain.

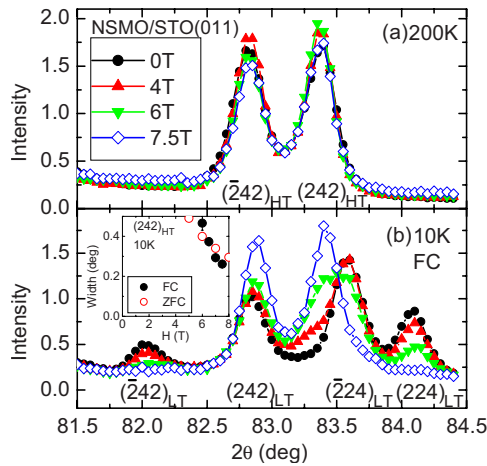


FIG. 2. (Color online) Intensity profile around 242 Bragg reflection measured at (a) 200 and (b) 10 K. The intensity was normalized so that the integrated intensity is constant when the magnetic field is applied. The inset for panel (b) shows the magnetic field dependence of the peak width of $(242)_{HT}$ component measured at 10 K with the field-cooled (FC) and zero-field-cooled (ZFC) procedures.

incides with T_A in a heating run in zero field.

In the present study, we observed clear phase coexistence of the HT phase and LT phase under the conditions of high magnetic field and low temperature. This remnant HT phase is found to originate from the large stress induced at the twin-2 domain boundary, and the LT-phase domain size is estimated from the detailed measurement of the LT-HT ratio as a function of temperature and magnetic field, as will be shown later.

Epitaxial films were grown by the pulsed laser deposition (PLD) method.⁸ The thickness of the NSMO film for this study was 80 nm, while no essential thickness dependence ranging from 50 to 110 nm was observed in transport and magnetic properties.⁸ First, we investigated transport properties of the sample with a standard four-probe method with 5 T magnetic property measurement system and 9 T physical property measurement system (Quantum Design). Figure 1 displays temperature dependence of resistivity measured along the $[100]$ axis by applying various magnetic fields with field-cooling and field-warming processes. The film has a clear first-order insulator-metal phase transition. T_{MI} and the resistivity in the insulating phase decreases as the field increases, which is naively understood in terms of the stabilization of the ferromagnetic spin arrangement and the resulting increase in the hopping probability.

X-ray diffraction experiment with photon energies of 12 and 14 keV in magnetic fields was carried out at BL-3A and BL-16A1 of the Photon Factory, KEK, Japan. A large two-circle diffractometer attached to an 8 T superconducting magnet was installed to these beamlines for this experiment; in the present configuration, the magnetic field was applied perpendicular to both $[011]$ and the scattering vector, which depends on the domain because the NSMO/STO has intrinsic twin structures, twin-1 and twin-2.

Figure 2 shows the intensity profiles around 242 Bragg reflection measured at (a) 200 and (b) 10 K with various magnetic fields. A magnetic field was applied in the FM

phase, and a field-cooled (FC) process was made for the measurements. Each plot shows the integrated intensity with respect to the diffractometer angle ω , and the figure shows the integrated intensities as a function of 2θ . Little change in the magnetic field is observed at 200 K. In panel (a), only two peaks corresponding to twin-1 are seen. According to the lattice parameters at zero field,⁹ the lower angle peak can be assigned to $(\bar{2}42)_{HT}$ and $(\bar{2}24)_{HT}$ and the higher angle to $(242)_{HT}$ and $(224)_{HT}$. Here, the suffix HT represents the indices in the lattice parameters for the HT phase. The relation $b=c$ in the HT phase makes the peak positions of hkl and $h\bar{l}k$ identical. In panel (b), there are four peaks related to both twin-1 and twin-2 in the zero-field profile. They are assigned to $(\bar{2}42)_{LT}$, $(242)_{LT}$, $(\bar{2}24)_{LT}$, and $(224)_{LT}$, from lower to higher angles, respectively. These low-temperature profiles had little temperature dependence up to 60 K, meaning that there is no significant change in the shape of unit cell or domain ratio below 60 K. The magnetic field prominently affected these peaks at low temperature. At 4 T, a bump appears at the left side of the $(\bar{2}24)_{LT}$ peak, and the intensity of $(224)_{LT}$ reflection decreases. The bump increases its intensity as the magnetic field increases, and at 7.5 T, the profile becomes almost identical to that at 200 K. The peak width, or the inverse correlation length, of the magnetic field-induced HT-phase peak $(242)_{HT}$ is shown in the inset of Fig. 2(b) as a function of the magnetic field. The width becomes broader, or the correlation length becomes shorter, as the field decreases to 4 T.

Superlattice reflections corresponding to the CE-OO phase are observed on the reciprocal lattice points of $\sqrt{2} \times 2\sqrt{2} \times 2$ unit cell for the LT-phase lattice parameters, as reported previously under zero field.¹⁰ These reflections are also observed in the magnetic field of up to 7 T. The temperature dependence of the integrated intensity of $(1/49/42)_{LT}$ superlattice and the $(224)_{LT}$ Bragg reflections was measured in order to investigate the T_{CE} and T_A values, respectively, in various magnetic fields; the transition temperature observed in lattice parameter, which is given by the positions of Bragg reflections, is higher one of T_{CE} or T_A , and that observed with superlattice reflection is T_{CE} .¹⁰ Below 4 T, the transition temperature T_A differs from T_{CE} , while they merge into one above this field. These features are summarized into a phase diagram shown in Fig. 3. The A-OO region decreases as the magnetic field increases. Above the crossing field, phase separation (represented by the shade) appears as seen in Fig. 2(b). At 4 T, $(242)_{HT}$ appears as a bump, $(242)_{HT}$ and $(\bar{2}24)_{LT}$ are comparable at 6 T, and the HT phase is dominant at 7.5 T. It should be noted that the T_{CE} at 4 T is 130 K; thus, no effect of the substrate transition at 105 K is expected on this phase separation phenomena.

Here we discuss how the phase separation state occurs in the film. Either ferro- or antiferro-orbital ordering in a film system on (011) substrates requires the shear-mode lattice distortion¹⁰ shown in the inset of Fig. 1. This mode of distortion, called the q_2 mode, makes lattice parameters b and c different. In an NSMO/STO film, twin-2 occurs at the HT-LT-phase transition, as shown in Fig. 2(b). In such a twinned system, there must be martensitic domain walls, which entail a large stress. In many bulk martensite transition systems, the

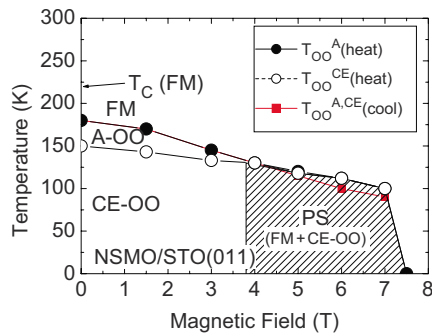


FIG. 3. (Color online) Temperature–magnetic field phase diagram for NSMO/STO(011). The magnetic field was parallel to the $[11\bar{1}]$ or $[1\bar{1}1]$ direction (depending on the domain). The magnetic field was applied in the FM phase, and transition temperatures were measured in both cooling and warming runs. PS represents the phase segregated state of FM and CE phases.

stress is often released by changing the shape of the crystal or making dislocations.¹¹ However, the former cannot happen in a film system because the substrate prohibits accumulation of the change in lattice parameters into a change in the size or shape of the whole sample. The latter also is not the case because the maximum translational displacement caused by the HT-LT transition, calculated as the thickness of the film multiplied by the tilt angle, is about 4 Å, less than the d spacing of $[0\bar{1}1]$. Only zero or one dislocation plane is expected. Therefore, a large stress that disallows the q_2 mode lattice distortion is induced around the domain wall. In turn, the orbital ordering is also suppressed. This situation is depicted in Figs. 4(a) and 4(b).

According to this scenario, no induced HT phase is expected in twin-2 free films. One such example is $\text{Pr}_{0.55}(\text{Ca}_{0.8}\text{Sr}_{0.2})_{0.45}\text{MnO}_3$ film on (011) surface of $[(\text{LaAlO}_3)_{0.3}(\text{SrAl}_{0.5}\text{Ta}_{0.5}\text{O}_3)_{0.7}]$ substrate, which has a charge-ordering transition at 160 K.¹² Our recent structural study on this film shows neither twin-2 nor any signature of an induced HT phase.¹³ This result supports the formation of the interfacial HT phase.

One of the intriguing facts seen in the phase diagram is the coincidence of the magnetic field where the phase coexistence starts and the crossing field of T_A and T_{CE} . This coincidence suggests that the $3d$ electronic state affects the martensitic transition. In the rest of this Rapid Communication, we discuss the relationship between the $3d$ electronic state and the phase coexistence.

Under the assumption that the HT phase at the low temperatures is located in the domain wall, its volume fraction is proportional to the thickness of the domain wall multiplied by the number density of the domain walls, the latter is inverse of the size of LT domains corresponding to twin-2, while the former is the size of the HT phase itself. The number of the LT domain, which equals to the number of domain wall, is fixed at the HT-LT transition point where the nucleation of the LT phase happens. When a LT domain vanishes, two domain boundaries collide with each other while a LT domain repels the other variant in order to minimize the elastic energy in the domain wall. As a result, the number of LT domains is decreased only when the thickness of the in-

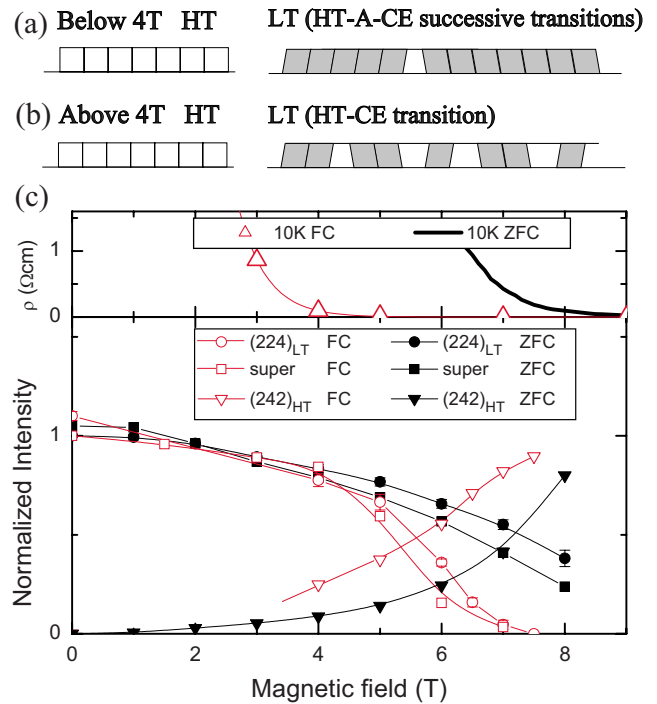


FIG. 4. (Color online) (a) Schematic view of the film at (left) high temperature and (right) low temperature for the cooling field below 4 T; (b) those for the cooling field above 4 T. The actual in-plane LT domain size is larger than 300 nm, the resolution limit of the experiment. (c) Volume fraction of the LT phase estimated by $(224)_{\text{LT}}$ intensity (circles) and the superlattice intensity (squares) measured at 10 K with field cool (open symbols) and zero-field cool (closed symbols) as a function of magnetic field, together with the HT-phase fraction by $(242)_{\text{HT}}$ intensity. Electric resistivity at 10 K in the field cool (open triangles) and zero-field cool (solid lines) is also presented.

terfacial HT phase diverges if we neglect the pinning of the domain boundary movement. This is why the number of the LT domain is conserved. The almost zero HT-phase volume under zero field at low temperature suggests that the domain wall is narrow. As the magnetic field increases, the ferromagnetic HT phase is energetically more favored; hence, the wall thickness grows. The gradual increase in the HT volume fraction under the ZFC condition, presented in Fig. 4(c), and the growth of the correlation length of HT phase for the ZFC case, in Fig. 2 inset, both support the picture.

Figure 4(c) shows the magnetic field dependence of both HT- and LT-phase fractions in the FC and ZFC processes. The sudden increase (decrease) in the HT (LT) phase and the associated coexistent behavior at 4 T observed in the FC process are puzzling at first sight because the lattice distortions in A-OO phase and CE-OO phase are alike and thus energetically similar, which leads to similar thickness of the interfacial HT phase for above and below the cooling field of 4 T. We thus have to seek another mechanism, the increase in the number of domains, as the cause. Based on the sudden decrease of LT fraction in HT-CE transition case observed in Fig. 4(c), the LT domain size made at T_{CE} is found to be much smaller than that made at T_A . This situation is illustrated in Figs. 4(a) and 4(b).

Various differences are observed in resistivity and structural property between the ZFC and the FC processes. As can be seen in Fig. 4(c), the magnetic field dependence of the resistivity measured at 10 K with the FC process is much smaller than that with the ZFC process under high magnetic fields, whereas they are the same at 0 T. The magnetic field dependences of the volume ratio between the HT phase and LT phase measured with the FC and ZFC processes significantly differ from each other [Fig. 4(c)], while those of the width of the $(242)_{\text{HT}}$ peak measured at 10 K are very similar [inset of Fig. 2(b)]. All these features are well understood with the above-mentioned mechanism. The peak width of the induced HT phase reflects the thickness of the boundary, which is dominated by the relationship between the elastic energy and the energy gain from the HT-LT-phase change. Thus, the same thickness is expected for the same temperature and magnetic field regardless of the procedure to reach the condition. The resistivity difference implies that the FC procedure gives larger fraction of the metallic HT phase than the ZFC process in high magnetic fields. This result is consistent with the volume fraction obtained by the Bragg peak intensities. As described above, this difference is interpreted to be caused by the different size of the LT domains.

Finally, we discuss the origin of the difference in domain size. We propose a model where the domain size of the or-

bitally ordered phase is dominated by the range of the electronic movement or itinerancy. The A-OO phase has high electric conductivity in the c plane,¹⁴ which means that the e_g electrons in the A-OO phase travel around nearly freely in the plane. At the HT-A transition temperature, one large orbitally ordered plane is established in a short time, and it distorts neighboring layers and forms a large domain. In contrast, the electrons in the CE-OO phase form zig-zag chains and the electron movement is confined in one-dimensional chains. At the HT-CE transition temperature, the zig-zag chain along the $[110]_{\text{HT}}$ and $[101]_{\text{HT}}$ directions grows independently and forms large numbers of small domains. Note that both transitions are first-order transitions; therefore, once the nucleation starts, the transition runs over a large volume with the speed of lattice vibration. In summary, the difference in ordering process is regarded as difference in speed of crystallization of electronic system that alters the domain size.

The authors thank T. Fujii and A. Asamitsu for the use of the 9T-PPMS system and K. Hagita for valuable discussions. This work was supported in part by a grant-in-aid for scientific research from MEXT, Japan and by the Sumitomo foundation.

*Present address: RIKEN, Hirosawa, Wako 351-0198, Japan.

¹J. Q. Li, *J. Appl. Phys.* **90**, 637 (2001).

²Y. Tokunaga, T. J. Sato, M. Uchida, R. Kumai, Y. Matsui, T. Arima, and Y. Tokura, *Phys. Rev. B* **77**, 064428 (2008).

³Y. Tokura and N. Nagaosa, *Science* **288**, 462 (2000).

⁴E. Dagotto, *New J. Phys.* **7**, 67 (2005).

⁵Several papers on L -edge resonant x-ray scattering on manganites report that $3d$ orbital ordering in manganites is strongly coupled with the lattice. For example, see S. B. Wilkins *et al.*, *Phys. Rev. B* **71**, 245102 (2005).

⁶V. Podzorov, B. G. Kim, V. Kiryukhin, M. E. Gershenson, and S.-W. Cheong, *Phys. Rev. B* **64**, 140406(R) (2001).

⁷K. H. Ahn, T. Lookman, and A. R. Bishop, *Nature (London)* **428**, 401 (2004).

⁸Y. Ogimoto, M. Nakamura, N. Takubo, H. Tamaru, M. Izumi,

and K. Miyano, *Phys. Rev. B* **71**, 060403(R) (2005).

⁹Y. Wakabayashi, D. Bizen, H. Nakao, Y. Murakami, M. Nakamura, Y. Ogimoto, K. Miyano, and H. Sawa, *Phys. Rev. Lett.* **96**, 017202 (2006).

¹⁰Y. Wakabayashi, D. Bizen, Y. Kubo, H. Nakao, Y. Murakami, M. Nakamura, Y. Ogimoto, K. Miyano, and H. Sawa, *J. Phys. Soc. Jpn.* **77**, 014712 (2008).

¹¹C. W. Wayman, *Introduction to the Crystallography of Martensitic Transformations* (Macmillan, New York, 1964).

¹²N. Takubo, Y. Ogimoto, M. Nakamura, H. Tamaru, M. Izumi, and K. Miyano, *Phys. Rev. Lett.* **95**, 017404 (2005).

¹³Y. Wakabayashi, N. Takubo, K. Miyano, and H. Sawa, *Eur. Phys. J. Spec. Top.* **167**, 67 (2009).

¹⁴M. Nakamura, M. Izumi, N. Ogawa, H. Ohsumi, Y. Wakabayashi, and K. Miyano, *J. Phys. Soc. Jpn.* **73**, 2802 (2004).